

Article

Acridine-Triphenylamine Based Hole-Transporting and Hole-Injecting Material for Highly Efficient Phosphorescent-Based Organic Light Emitting Diodes

Ramanaskanda Braveenth ¹ , Il-Ji Bae ², Yan Wang ³, Soo Hyeon Kim ¹, Miyoung Kim ^{2,*} and Kyu Yun Chai ^{1,*} 

¹ Division of Bio-Nanochemistry, College of Natural Sciences, Wonkwang University Iksan City, Chonbuk 570-749, Korea; braveenth.czbt@gmail.com (R.B.); qazhan522@hanmail.net (S.H.K.)

² Nano-Convergence Research Center, Korea Electronics Technology Institute, Jeonju 54853, Korea; ijbae@keti.re.kr

³ Department of Chemistry and Chemical Engineering, Hebei Normal University for Nationalities, Chengde 067000, China; 13091357999@163.com

* Correspondence: miy1kim@keti.re.kr (M.K.); geuyoon@wonkwang.ac.kr (K.Y.C.); Tel.: +82-632-190-011 (M.K.); +82-638-506-230 (K.Y.C.)

Received: 25 June 2018; Accepted: 17 July 2018; Published: 18 July 2018



Featured Application: We have identified our synthesized TPA-1A material can apply as hole injecting and hole transporting material for PhOLEDs applications.

Abstract: In this study, triphenylamine-based hole-transporting material 4-(9,9-diphenylacridin-10(9H)-yl)-N-(4-(9,9-diphenylacridin-10(9H)-yl) phenyl)-N-phenylaniline (TPA-1A) was designed and synthesized by using single-step Buchwald–Hartwig coupling reaction with higher yield percentage of 76%. Our synthesized TPA-1A showed excellent thermal stability, with a higher glass transition temperature of 176 °C and decomposition temperature of 474 °C at 5% weight reduction. TPA-1A based green phosphorescent organic light emitting diodes (PhOLED) device was fabricated to investigate the device properties and compare it with the similar reference *N,N'*-Di(1-naphthyl)-*N,N'*-diphenyl-(1,1'-biphenyl)-4,4'-diamine (NPB) based device. The TPA-1A-based PhOLED demonstrated an excellent current and power efficiency of 49.13 cd/A and 27.56 lm/W, respectively. Moreover, TPA-1A demonstrated better hole injection efficiencies as well. The overall efficiencies were better than the reference NPB-based device.

Keywords: hole-transporting material; organic electronic materials; acridine; green phosphorescent; higher efficiency

1. Introduction

Organic light emitting diodes (OLEDs) have given dramatic development in display technology and printed flexible electronics because of their efficiency enhancement while showing advantages of lower power consumption, high brightness, and contrast. The general OLED structure consists of two electrodes, namely, an anode and cathode at both ends. There is a hole-injecting layer (HIL), hole-transporting layer (HTL), emission layer (EML), electron-transporting layer (ETL), electron-injecting layer (EIL) embedded between two electrodes, the anode and cathode, which is known as a multilayer OLED structure. Multilayer OLED devices have improved the quantum efficiency when compared to single-layer devices [1–4]. Hole-transporting materials (HTM) play a major role to transporting holes from the anode to the emission layer and providing charge balance to prevent efficiency roll-off, since the hole transportation process faces critical issues, like thermal

instability, lower hole mobility, and hole injection barrier [5–7]. Small molecular hole-transporting materials expressed crystallization features during long operation times, but they showed shallow HOMO energy levels as an advantage.

To overcome those issues, there are many hole-transporting materials synthesized with different structural modifications. Arylamine, spiro derivatives, and carbazole-based molecular structures have been extensively used as hole-transporting materials for their excellent electron-donating capability [8–13]. The most abundantly used HTMs, 4,4,4-tris(*N*-carbazolyl) triphenylamine (TCTA), *N,N'*-Di(1-naphthyl)-*N,N'*-diphenyl-(1,1'-biphenyl)-4,4'-diamine (NPB) and *N,N'*-Bis(3-methylphenyl)-*N,N'*-diphenylbenzidine (TPD), have been communicated with higher quantum efficiencies. However, NPB and TPD materials revealed poor thermal and morphological stabilities, and TCTA expressed inferior hole mobility [14–17]. The OLED device degradation mechanism is not fully studied, but several reports indicate that major morphological changes of the amorphous hole-transporting layer (HTL) [18,19].

One of the largest obstacles in the development of highly efficient and stable phosphorescent organic light emitting diode (PhOLED) is the design and synthesis of effective hole-transporting materials, which should possess higher hole mobility with lower injection barrier and stable morphological properties. Especially, triphenylamine (TPA) and its derivatives received an astonishing achievement in many optoelectronic studies, like perovskite solar cells (PSCs), OLEDs, and organic field effect transistors (OFET), in the form of small molecules and oligomers. There are many advantages associated with TPA moieties, which are electron-donating, low ionization potential, high hole mobility, and have a stable morphology and thermal properties. Predominantly, electron contribution depends on nitrogen atoms in the TPA and TPA-based moieties in which the N atom can be oxidized and transport positive charges (holes) adequately. Moreover, TPA groups can further modify with different substituent groups to extend the conjugation length which enhances the electronic properties additionally [20–29].

Acridine (ACR)-based molecules have been extensively used in thermally-activated delayed-fluorescence (TADF) emitters and host materials, as electron-donating units and hole-transporting materials in solar cells and OLED applications. Although ACR can be utilized as hole-transporting material in OLED applications due to the presence of electron-donating nitrogen atoms at the 10th position in between two phenyl rings, a structure that resembles the TPA molecule, but with two phenyl rings of TPA connected via a methylene bridge to form a hexagonal ACR molecule. The ACR molecule is more rigid than the TPA molecule, which will be useful in HTM applications in OLEDs. Moreover, free rotating phenyl groups at the 9th position can enhance the rigidity, thermal stability, and also prevent pi-pi stacking over molecules. This observation will give a better result as a hole-transporting material when compared to carbazole-based molecules [30–37].

In this study, we have designed and synthesized a hole-transporting material with a triphenylamine core and diphenyl acridine moieties, which was anticipated to show higher quantum efficiencies with stable thermal properties.

2. Materials and Methods

2.1. Materials

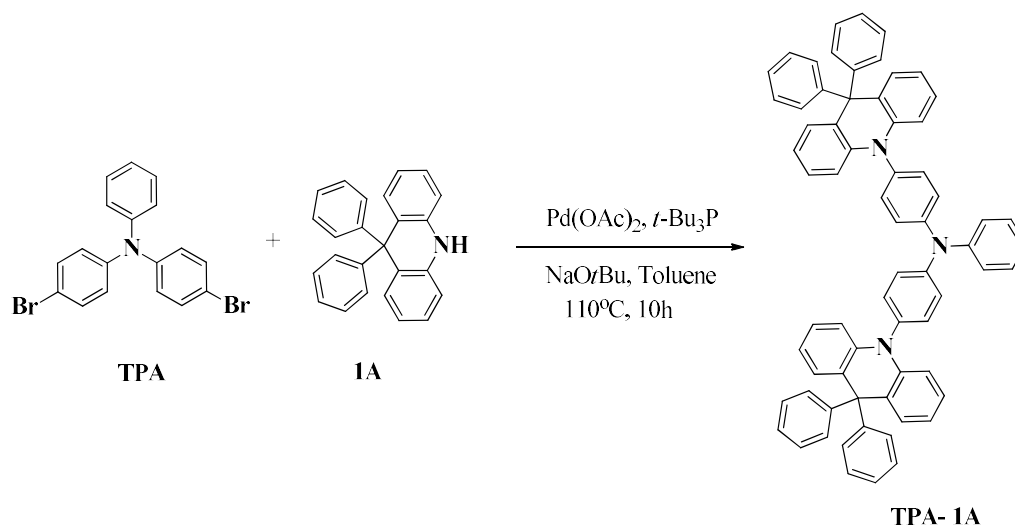
All reagents and solvents were acquired from commercial suppliers. TPA and 1A were purchased from TCI chemicals (Seoul, Korea). Toluene, n-hexane, and dichloromethane were purchased from SK Chemicals (Gyeonggi-do, Korea). Toluene was distilled from sodium/benzophenone before use. Analytical thin layer chromatography (TLC) was completed by using aluminum-backed Merck Kieselgel 60 coated plates (Seoul, Korea). Column chromatography was performed using silica gel with a mesh size of 200–300.

2.2. Instrumentation

^1H and ^{13}C NMR spectra were recorded using a JEON JNM-ECP FT-NMR spectrometer (Peabody, MA, USA) operating at 500 MHz. Absorbance spectra were obtained using a SINCO S-4100 ultraviolet visible (UV–VIS) spectrophotometer (SINCO, Seoul, Korea). The energy of the band gap (E_g) was estimated from the onset wavelength of the UV–VIS absorbance spectra. Photoluminescence (PL) spectra were recorded using a HR800 spectrofluorimeter (Horiba Jobin Yvon, Paris, France). The triplet energy level (E_T) was determined from the onset wavelength of the emission spectra at 77 K in tetrahydrofuran (THF). The HOMO (highest occupied molecular orbital) level was calculated by the AC-2 method using a photoelectron spectrometer (RIKEN, Saitama, Japan). The LUMO (lowest unoccupied molecular orbital) level was estimated by adding the band gap energy to the obtained HOMO energy. OLED devices were fabricated by a thermal evaporating system (5×10^{-7} torr pressure) (Sunicel plus, Seoul, Korea). Current density-voltage-luminescence (J-V-L) efficiencies were recorded by an OLED I-V-L test system (Polarmix M6100, Suwon, Korea). The electroluminescence (EL) spectra analysis was obtained by using a spectroradiometer (Konica Minolta CS-2000, Tokyo, Japan). Thermal gravimetric analysis (TGA) and differential scanning calorimetry (DSC) were organized by using SDT Q600 V20.9 Build 20 and DSC Q200 V24.9 Build 121 (TA Instruments, New Castle, DE, USA) instruments with a heating rate of $10\text{ }^\circ\text{C}/\text{min}$ under an inert atmosphere. Mass spectrometry analysis was carried out using a Xevo TQ-S spectrometer (Waters, Milford, MA, USA). Elemental analysis (EA) was measured by an IT/flash/2000 elemental analyser (Thermo Fisher Scientific, Loughborough, UK).

2.3. Synthesis of 4-(9,9-Diphenylacridin-10(9H)-yl)-N-(4-(9,9-diphenylacridin-10(9H)-yl)phenyl)-N-phenylaniline (TPA-1A)

A mixture of 4-bromo-N-(4-bromophenyl)-N-phenylaniline (TPA, 2 g, 4.96 mmol), 4-(9,9-diphenylacridin-10(9H)-yl)-N-(4-(9,9-diphenylacridin-10(9H)-yl)phenyl)-N-phenylaniline (1A, 3.47 g, 10.40 mmol), $\text{Pd}(\text{OAc})_2$ (0.03 g, 0.15 mmol), sodium tert-butoxide (1.81 g, 18.80 mmol), 10% tri-tert-butylphosphine in toluene (0.70 mL, 3.5 mmol) and 100 mL of anhydrous toluene were added in a two-neck 150 mL round bottom flask equipped with condenser. The mixture was then stirred at $110\text{ }^\circ\text{C}$ for 10 h under a nitrogen atmosphere. The residues were extracted with dichloromethane ($3 \times 30\text{ mL}$) and deionized water (60 mL). The organic layer was collected, dried over anhydrous sodium sulphate and concentrated through a rotary evaporator. Finally, the crude material was separated using a silica column with an *n*-hexane: dichloromethane (5:1 to 1:1) gradient-based mobile phase to achieve the pure TPA-1A target molecule. Synthesize route of TPA-1A is illustrated in Scheme 1.



Scheme 1. Synthesis of hole-transporting material TPA-1A. 4-(9,9-diphenylacridin-10(9H)-yl)-N-(4-(9,9-diphenylacridin-10(9H)-yl)phenyl)-N-phenylaniline, Yield: 76%; white solid; ^1H NMR (500 MHz,

CDCl_3) δ 7.32–7.35 (t, $J = 10$ Hz, 1H), 8.22–8.26 (m, 9H), 7.09–7.12 (m, 2H), 6.97–6.98 (m, 4H), 6.92–6.93 (d, $J = 8.5$ Hz, 2H), 6.87–6.88 (d, $J = 8.5$ Hz, 4H), 6.55–6.57 (d, $J = 8$ Hz, 2H); ^{13}C NMR (500 MHz, CDCl_3) δ 147.26, 146.44, 142.40, 130.47, 130.00, 129.90, 129.72, 127.67, 126.93, 126.33, 125.28, 116.12, 114.13; MS (APCI) m/z : 907.83 for $\text{C}_{68}\text{H}_{49}\text{N}_3$ [(M + H) $^+$]. Anal. Calcd for $\text{C}_{68}\text{H}_{49}\text{N}_3$ (%): C, 89.93; H, 5.44; N, 4.63. Found: C, 89.86; H, 5.40; N, 4.71.

2.4. OLED Fabrication and Characterization

Green phosphorescence based OLED devices (PhOLEDs) were fabricated with our new hole-transporting material (TPA-1A) to investigate the efficiencies when compare to NPB-based reference device. A 150 nm thickness substrate was subjected to ultra-sonication with isopropyl alcohol for 10 min, and followed by deionized water treatment. Then, ultraviolet and ozone treatment was held further. A thermal evaporating system with the pressure of 5×10^{-7} torr was used to fabricate the organic layer-embedded OLED devices. Consequently, deposited devices were encapsulated with glass covers and the size of the device was 2 mm².

3. Results and Discussions

3.1. Thermal and Morphological Properties

The thermal stabilities of TPA-1A were investigated by TGA and DSC measurements; these data are shown in Figure 1 and summarized in Table 1. TPA-1A exhibited a high glass transition temperature of 176 °C, while demonstrating a high decomposition temperature of 474 °C for 5% weight reduction. The observed values are more suitable for thermally stable device applications and which enhance the morphological properties during device fabrication. Consequently, our materials revealed a higher melting point of 351 °C. TPA-1A showed outstanding thermal properties than well-known reference hole-transporting materials NPB (98 °C) and TPD (65 °C) due to its highly conjugated structure and rigid diphenyl acridine moiety attached to the triphenylamine central core [38,39].

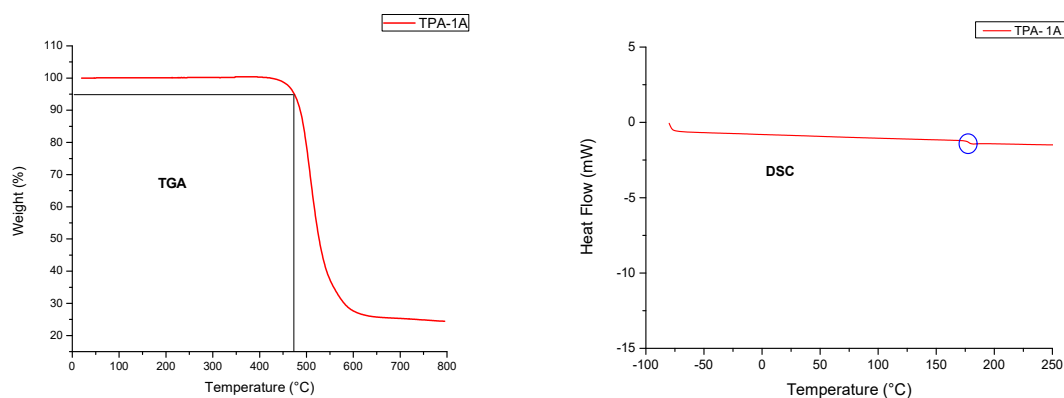


Figure 1. Thermal gravimetric analysis (TGA) and differential scanning calorimetry (DSC) distribution of TPA-1A.

The morphological studies of films are supported by scanning electron microscope (SEM) imagery and depicted in Figure 2. We could observe a well-defined multilayer structure with visible interfaces. Each layer shows proper contact with their adjacent layer, which helps to enhance the device efficiencies through proper charge transportation.

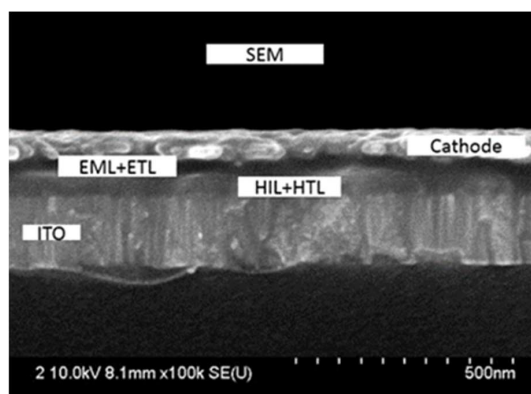


Figure 2. Scanning electron microscope (SEM) images of the TPA-1A-based device cross-section.

3.2. Electrochemical and Photophysical Properties

The HOMO energy level of TPA-1A was -5.78 eV, and showed little lower energy value with the NPB material (-5.5 eV). The HOMO energy level is lying between the anode (-4.80 eV) and the emission layer (-5.90 eV). The suitable HOMO energy level helps to transport holes effectively from the anode (Table 1). The HOMO energy difference between TPA-1A and the emission layer is 0.1 eV, while the energy difference of NPB is 0.4 eV. Lowering the energy difference can enhance the efficiencies through providing an effective hole-hopping path. The LUMO energy was -2.45 eV, which was calculated by adding the band gap to the HOMO energy. The LUMO energy level is higher than that of the electron transporting layer (-2.80 eV), which is beneficial for acting as an electron blocking layer. The frontier molecular orbital (FMO) energy levels were matched with the adjacent layers of the fabricated OLED device to ensure the effective charge transportation.

Table 1. Thermal, photophysical, and electrochemical properties of 4-(9,9-Diphenylacridin-10(9H)yl)-N-(4-(9,9-diphenylacridin-10(9H)-yl)phenyl)-N-phenylaniline (TPA-1A).

HTM	T _g ^a (°C)	T _d ^b (°C)	UV-Vis ^c (nm)	PL max ^d (nm)	HOMO ^e (eV)	LUMO ^f (eV)	E _g ^g (eV)	E _T ^h (eV)
TPA-1A	176	474	319	425	-5.78	-2.45	3.33	2.58

^a Glass transition temperature; ^b Decomposition temperature at 5% weight reduction; ^c UV absorption wavelength; ^d Photoluminescent emission; ^e Highest occupied molecular orbital energy; ^f Lowest unoccupied molecular orbital energy; ^g Energy band gap; ^h Triplet energy.

Figure 3 describes the UV-VIS absorption and photoluminescence (PL) spectra of TPA-1A, which showed a maximum absorption peak at 319 nm. The above absorption is attributed to the π - π^* transition of the aromatic rings. The band gap value of TPA-1A was 3.33 eV, which was calculated from the on-set absorption at 372 nm. We did not notice any prominent absorption in the visible region.

The PL emission at room temperature revealed a maximum at 425 nm. The triplet energy was 2.58 eV, which was measured from the low temperature PL emission (77 K) at 481 nm and which is lower than that of spiro-based molecules.

Commonly, spirobifluorene without other molecular attachment has a higher triplet energy of 2.87 eV, when another molecule attaches via the para position leading to lowering the triplet energy around 2.52 eV compared to the ortho position (2.77 eV). In the case of the ortho position, pi electron delocalization is restricted, which has a higher triplet energy. Moreover, when a molecule attached through the para position makes a long conjugation length by delocalizing more electrons, it affects the triplet energy. In our molecule, acridine attached with triphenyl amine through the para position which extended the conjugation length while decreasing the triplet energy [40]. Cho et al. reported on a green phosphorescence OLED with the higher triplet energy material

N,N,N',N'-tetraphenyl-spiro(cyclopenta[de]fluorene-1,5,9',9''-bifluorene)-2',7'-diamine (DSBF-DPA) (2.44 eV), which exhibited an external quantum efficiency of 16.5%, higher than that of a similar NPB-based device (10.4%). The author revealed that the higher triplet energy can prevent the triplet exciton which come from the emission material. NPB, which showed a lower triplet energy (2.3 eV) than the green dopant Ir(ppy)₃ (2.4 eV), led to a drop in device efficiency [41].

Triplet energy is an important phenomenon in organic devices to improve their efficiencies. TPA-1A showed a slightly higher triplet energy of 2.58 eV compared to NPB, which can lead to facilitating effective triplet exciton blocking to enhance the device efficiencies.

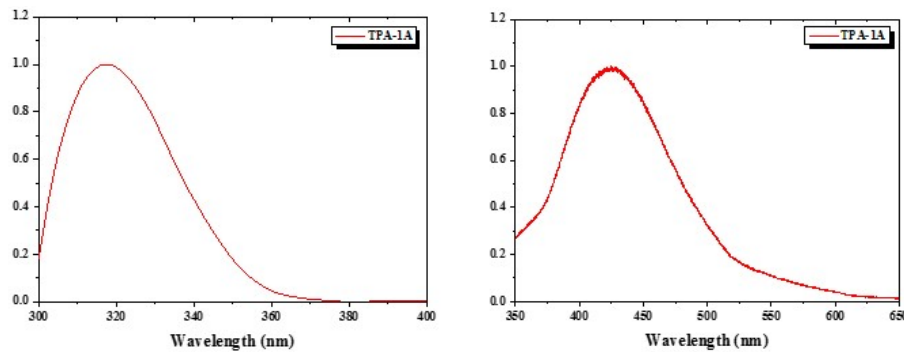


Figure 3. Ultraviolet visible (UV–VIS) absorption and photoluminescent spectra of TPA-1A.

3.3. Device Characteristics

To investigate the hole-injection and hole-transporting properties, we have fabricated two green phosphorescence OLED devices with TPA-1A as the hole-transporting material and hole-injecting materials. The energy diagram of both device structures are depicted in Figure 4. The device structure of the TPA-1A hole-transporting layer (HTL) was indium tin oxide (ITO) (150 nm)/1,4,5,8,9,11-Hexaazatriphenylenehexacarbonitrile (HATCN) (10 nm)/HTL (15 nm)/4,4'-Bis(*N*-carbazolyl)-1,1'-biphenyl (CBP): 5 wt % Tris[2-phenylpyridinato-C_{2,N}]iridium(III) (Ir(ppy)₃)/bathophenanthroline (Bphen) (30 nm)/8-quinolinolato lithium (Liq) (1 nm)/aluminium (Al) (100 nm). ITO and Al were used as the anode and cathode, respectively. HATCN was the hole-injecting layer (HIL), while Liq was the electron injecting layer (EIL). The CBP host material was doped with green emitting Ir(ppy)₃. To compare the device efficiencies of TPA-1A, a NPB-based reference device with a similar structure was fabricated. Another device structure of TPA-1A as a hole-injecting layer was indium tin oxide (ITO) (150 nm)/HIL (10 nm)/HTL-NPB (15 nm)/4,4'-Bis(*N*-carbazolyl)-1,1'-biphenyl (CBP): 5 wt % Tris[2-phenylpyridinato-C_{2,N}]iridium(III) (Ir(ppy)₃)/bathophenanthroline (Bphen) (30 nm)/8-quinolinolato lithium (Liq) (1 nm)/aluminium (Al) (100 nm).

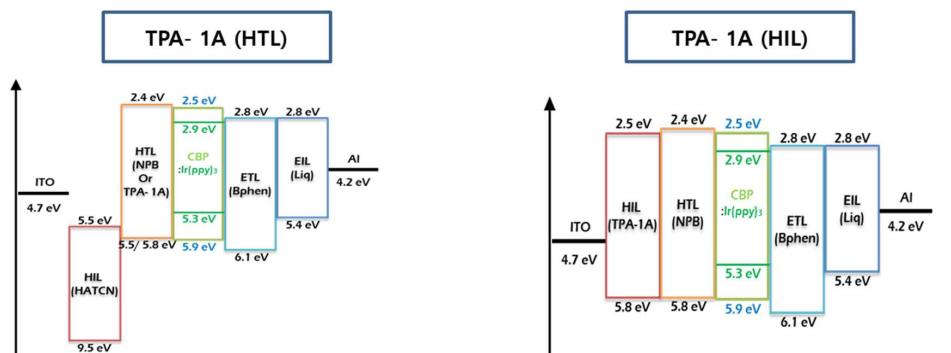


Figure 4. Energy diagram and device structure of TPA-1A-based Organic light emitting (OLED) devices.

The current density-voltage-luminescence (J-V-L) characteristics are depicted in Figure 5. The TPA-1A-based device showed a higher turn-on voltage of 4.4 V when compared to the NPB-based device (3.4 V). The green PhOLED device showed similar power efficiencies of 30.85 and 31.62 lm/W for NPB and TPA-1A, respectively, at turn-on voltage. The power efficiencies at 1200 cd/m² for TPA-1A was 27.56 lm/W, which is much higher than that of the reference NPB-based device (19.88 lm/W). The above results explained that the power efficiency of the TPA-1A-based device not only depends on the turn-on voltage, but also the balance of electrons and holes in the device.

The current efficiency of the TPA-1A-based green PhOLED at the turn-on voltage was 44.29 cd/A, but the NPB-based reference device showed lower efficiency of 33.38 cd/A. At 1200 cd/m², TPA-1A exhibited an excellent current efficiency of 49.13 cd/A when compared to NPB (27.21 cd/A). Consequently, the current efficiency of the TPA-1A-based device dramatically increased with the luminescence value of 1282 cd/m². Interestingly, the TPA-1A-based device showed an outstanding external quantum efficiency (EQE) of 13.74%, while the NPB-based reference device showed a lower EQE of 7.64%. We believe that the higher triplet energy of TPA-1A helped to improve the efficiencies when compared to the NPB-based device. All data are summarized in Table 2. As a result, the TPA-1A-based green PhOLED revealed excellent device efficiencies than the reference (NPB) device.

Additionally, we have studied the hole-injecting property of TPA-1A in which we used NPB as the hole-transporting material. The device characteristics and efficiencies are shown in Figure 5 and summarized in Table 2. The current efficiency was noticed as 37.09 cd/A, while the power efficiency was 32.37 lm/W at the turn-on voltage (3.6 V). Consequently, the TPA-1A (HIL) device showed an external quantum efficiency of 14.59, 8.53% at the turn-on voltage and 1200 cd/m², respectively. TPA-1A (HIL) device exhibited better performance when compare to other devices which used HATCN as the hole-injecting layer with the NPB hole-transporting material. Finally, we found that overall performance of TPA-1A as a hole-transporting and hole-injecting material enhanced the device efficiencies.

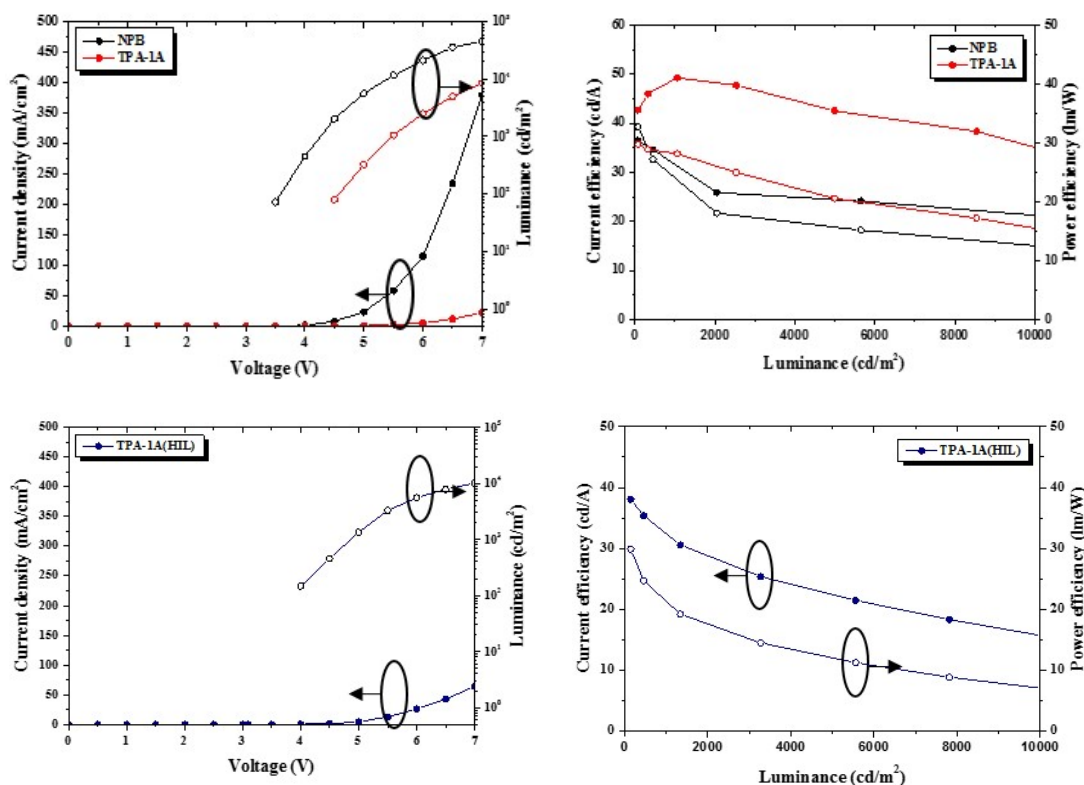


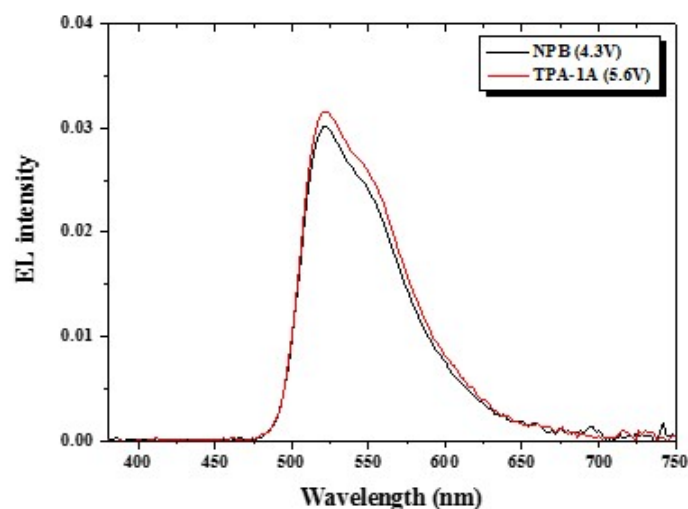
Figure 5. J-V-L, luminescence-current, and power efficiency curves of TPA-1A-based devices.

Table 2. Device properties of TPA-1A (HTL) with reference *N,N'*-Di(1-naphthyl)-*N,N'*-diphenyl-(1,1'-biphenyl)-4,4'-diamine NPB and TPA-1A (HIL).

Characteristic	TPA-1A (HTL)	NPB (Reference)	TPA-1A (HIL)
Current (mA)	0.006 ^a	0.006 ^a	0.01 ^a
	0.10 ^b	0.18 ^b	0.18 ^b
Current efficiency (cd/A)	44.29 ^a	33.38 ^a	37.09 ^a
	49.13 ^b	27.21 ^b	30.57 ^b
Power efficiency (lm/W)	31.62 ^a	30.85 ^a	32.37 ^a
	27.56 ^b	19.88 ^b	19.21 ^b
Luminescence (cd/m ²)	62.81 ^a	48.4 ^a	146.2 ^a
	1282 ^b	1197 ^b	1341 ^b
External quantum efficiency (EQE %)	15.50 ^a	13.39 ^a	14.59 ^a
	13.74 ^b	7.64 ^b	8.53 ^b
International Commission on Illumination CIE (x,y) ^b	0.33, 0.62	0.33, 0.63	0.34, 0.61

^a At turn-on voltage; ^b At 1200 cd/m².

The electroluminescence spectra of TPA-1A and NPB-based green PhOLEDs are shown in Figure 6. Both devices exhibited an identical EL emission peak, which was attributed to the CIE (x,y) colour coordinate values of 0.33, 0.62 and 0.33, 0.63 for TPA-1A- and NPB-based PhOLED, respectively.

**Figure 6.** Electroluminescent (EL) spectra of fabricated green PhOLEDs.

4. Conclusions

In summary, triphenylamine- and acridine-based hole-transporting material TPA-1A was designed and synthesized. The synthesized hole-transporting material showed excellent thermal stability due to its rigid acridine moiety on both sides of the triphenylamine central core. The current efficiency of TPA-1A was 49.13 cd/A, which is higher than the NPB-based reference device (27.21 cd/A). Our material manifested an excellent power efficiency of 27.56 lm/W at 1200 cd/m². Moreover, the external quantum efficiency of TPA-1A was 13.74%, while the reference NPB exhibited a lower efficiency of 7.64%. Furthermore, the hole injection properties of TPA-1A (HIL) were demonstrated by an outstanding external quantum efficiency of 14.59%. Triphenylamine-acridine derivatives enhanced the device properties to ensure the proper charge balance than the NPB-based device. TPA-1A is a good candidate for highly efficient and thermally stable OLED applications.

Author Contributions: K.Y.C. and R.B. designed the project; R.B. and S.H.K. synthesized and characterized the material; I.-J.B. and Y.W. fabricated the OLED device; M.K. supervised the device fabrication process; and R.B. analyzed and wrote the manuscript. All authors read and approved the final manuscript.

Funding: This research received no external funding.

Acknowledgments: This research was supported by Wonkwang University (2016).

Conflicts of Interest: The authors declare no conflict of interest.

References

1. Kochapradist, P.; Prachumrak, N.; Tarsang, R.; Keawin, T.; Jungsuttiwong, S.; Sudyoasuk, T.; Promarak, V. Multi-triphenylamine-substituted carbazoles: Synthesis, characterization, properties, and applications as hole-transporting materials. *Tetrahedron Lett.* **2013**, *54*, 3683–3687. [[CrossRef](#)]
2. Wolak, M.A.; Delcamp, J.; Landis, C.A.; Lane, P.A.; Anthony, J.; Kafafi, Z. High-Performance Organic Light-Emitting Diodes Based on Dioxolane-Substituted Pentacene Derivatives. *Adv. Funct. Mater.* **2006**, *16*, 1943–1949. [[CrossRef](#)]
3. Huh, D.H.; Kim, G.W.; Kim, G.H.; Kulshreshtha, C.; Kwon, J.H. High hole mobility hole transport material for organic light-emitting devices. *Synth. Met.* **2013**, *180*, 79–84. [[CrossRef](#)]
4. Usluer, O.; Demic, S.; Egbe, D.A.; Birckner, E.; Tozlu, C.; Pivrikas, A.; Sariciftci, N.S. Fluorene-Carbazole Dendrimers: Synthesis, Thermal, Photophysical and Electroluminescent Device Properties. *Adv. Funct. Mater.* **2010**, *20*, 4152–4161. [[CrossRef](#)]
5. Takizawa, S.Y.; Montes, V.A.; Anzenbacher, J.P. Phenylbenzimidazole-based new bipolar host materials for efficient phosphorescent organic light-emitting diodes. *Chem. Mater.* **2009**, *21*, 2452–2458. [[CrossRef](#)]
6. Kuwabara, Y.; Ogawa, H.; Inada, H.; Noma, N.; Shirota, Y. Thermally stable multilayered organic electroluminescent devices using novel starburst molecules, 4,4',4''-Tri (*N*-carbazolyl) triphenylamine (TCTA) and 4,4',4''-Tris (3-methylphenylphenylamino) triphenylamine (m-MTDATA), as hole-transport materials. *Adv. Mater.* **1994**, *6*, 677–679. [[CrossRef](#)]
7. Long, L.; Zhang, M.; Xu, S.; Zhou, X.; Gao, X.; Shang, Y.; Wei, B. Cyclic arylamines functioning as advanced hole-transporting and emitting materials. *Synth. Met.* **2012**, *162*, 448–452. [[CrossRef](#)]
8. Braveenth, R.; Bae, H.W.; Ko, I.J.; Qiong, W.; Nguyen, Q.P.B.; Jayashantha, P.G.S.; Kwon, J.H.; Chai, K.Y. Thermally stable efficient hole-transporting materials based on carbazole and triphenylamine core for red phosphorescent OLEDs. *Org Electron.* **2017**, *51*, 463–470. [[CrossRef](#)]
9. Okumoto, K.; Shirota, Y. Development of new hole-transporting amorphous molecular materials for organic electroluminescent devices and their charge-transport properties. *Mater. Sci. Eng. B* **2001**, *85*, 135–139. [[CrossRef](#)]
10. Braveenth, R.; Bae, I.J.; Han, J.H.; Qiong, W.; Seon, G.; Raagulan, K.; Yang, K.; Park, Y.H.; Kim, M.; Chai, K.Y. Utilizing a Spiro Core with Acridine- and Phenothiazine-Based New Hole-transporting materials for Highly Efficient Green Phosphorescent Organic Light-Emitting Diodes. *Molecules* **2018**, *23*, 713. [[CrossRef](#)] [[PubMed](#)]
11. Kim, S.H.; Jang, J.; Yook, K.S.; Lee, J.Y. Stable efficiency roll-off in phosphorescent organic light-emitting diodes. *Appl. Phys. Lett.* **2008**, *92*, 023513. [[CrossRef](#)]
12. Li, J.; Liu, D.; Li, Y.; Lee, C.S.; Kwong, H.L.; Lee, S. A high Tg carbazole-based hole-transporting material for organic light-emitting devices. *Chem. Mater.* **2005**, *17*, 1208–1212. [[CrossRef](#)]
13. Quinton, C.; Thiery, S.; Jeannin, O.; Tondelier, D.; Geffroy, B.; Jacques, E.; Berthelot, J.R.; Poriel, C. Electron-rich 4-substituted spirobifluorenes: Toward a new family of high triplet energy host materials for high-efficiency green and sky blue phosphorescent OLEDs. *ACS Appl. Mater. Interfaces* **2017**, *9*, 6194–6206. [[CrossRef](#)] [[PubMed](#)]
14. Chu, Z.; Wang, D.; Zhang, C.; Wang, F.; Wu, H.; Lv, Z.; Zou, D. Synthesis of spiro [fluorene-9,9'-xanthene] derivatives and their application as hole-transporting materials for organic light-emitting devices. *Synth. Met.* **2012**, *162*, 614–620. [[CrossRef](#)]
15. Feng, G.L.; Lai, W.Y.; Ji, S.J.; Huang, W. Synthesis of novel star-shaped carbazole-functionalized triazatruxenes. *Tetrahedron Lett.* **2006**, *47*, 7089–7092. [[CrossRef](#)]
16. Hou, X.Y.; Li, T.C.; Yin, C.R.; Xu, H.; Lin, J.; Hua, Y.R.; Huang, W. Stable hole-transporting molecular glasses based on complicated 9,9-diarylfuorenes (CDAFs). *Synth. Met.* **2009**, *159*, 1055–1060. [[CrossRef](#)]

17. Tsutsui, T. Progress in electroluminescent devices using molecular thin films. *Mrs Bull.* **1997**, *22*, 39–45. [[CrossRef](#)]
18. Park, J.Y.; Kim, J.M.; Lee, H.; Ko, K.Y.; Yook, K.S.; Lee, J.Y.; Baek, Y.G. Thermally stable triphenylene-based hole-transporting materials for organic light-emitting devices. *Thin Solid Films* **2011**, *519*, 5917–5923. [[CrossRef](#)]
19. Tong, Q.X.; Lai, S.L.; Chan, M.Y.; Lai, K.H.; Tang, J.X.; Kwong, H.L.; Lee, S.T. High Tg triphenylamine-based starburst hole-transporting material for organic light-emitting devices. *Chem. Mater.* **2007**, *19*, 5851–5855. [[CrossRef](#)]
20. Adachi, C.; Nagai, K.; Tamoto, N. Molecular design of hole transport materials for obtaining high durability in organic electroluminescent diodes. *Appl. Phys. Lett.* **1995**, *66*, 2679–2681. [[CrossRef](#)]
21. Karthikeyan, C.S.; Wietasch, H.; Thelakkat, M. Highly efficient solid-state dye-sensitized TiO₂ solar cells using donor-antenna dyes capable of multistep charge-transfer cascades. *Adv. Mat.* **2007**, *19*, 1091–1095. [[CrossRef](#)]
22. Tang, C.W.; VanSlyke, S.A.; Chen, C.H. Electroluminescence of doped organic thin films. *J. Appl. Phys.* **1989**, *65*, 3610–3616. [[CrossRef](#)]
23. Cias, P.; Slugovc, C.; Gescheidt, G. Hole transport in triphenylamine based OLED devices: From theoretical modeling to properties prediction. *J. Phys. Chem. A* **2011**, *115*, 14519–14525. [[CrossRef](#)] [[PubMed](#)]
24. Zhang, K.; Wang, L.; Liang, Y.; Yang, S.; Liang, J.; Cheng, F.; Chen, J. A thermally and electrochemically stable organic hole-transporting material with an adamantane central core and triarylamine moieties. *Synth. Met.* **2012**, *162*, 490–496. [[CrossRef](#)]
25. Burroughes, J.H.; Bradley, D.D.C.; Brown, A.R.; Marks, R.N.; Mackay, K.; Friend, R.H.; Holmes, A.B. Light-emitting diodes based on conjugated polymers. *Nature* **1990**, *347*, 539–541. [[CrossRef](#)]
26. Choi, H.; Ko, H.M.; Ko, J. Stable and efficient star-shaped hole-transporting materials with EDOT moiety as side arm for perovskite solar cells. *Dyes Pigm.* **2016**, *126*, 179–185. [[CrossRef](#)]
27. Tao, Y.; Wang, Q.; Yang, C.; Zhong, C.; Qin, J.; Ma, D. Multifunctional Triphenylamine/Oxadiazole Hybrid as Host and Exciton-Blocking Material: High Efficiency Green Phosphorescent OLEDs Using Easily Available and Common Materials. *Adv. Funct. Mater.* **2010**, *20*, 2923–2929. [[CrossRef](#)]
28. Agarwala, P.; Kabra, D. A review on triphenylamine (TPA) based organic hole transport materials (HTMs) for dye sensitized solar cells (DSSCs) and perovskite solar cells (PSCs): Evolution and molecular engineering. *J. Mater. Chem. A* **2017**, *5*, 1348–1373. [[CrossRef](#)]
29. Thelakkat, M. Star-Shaped, Dendrimeric and Polymeric Triarylaminines as Photoconductors and Hole Transport Materials for Electro-Optical Applications. *Macromol. Mater. Eng.* **2002**, *287*, 442–461. [[CrossRef](#)]
30. Torres, A.; Rego, L.G. Surface effects and adsorption of methoxy anchors on hybrid lead iodide perovskites: Insights for Spiro-MeOTAD attachment. *J. Phys. Chem. C* **2014**, *118*, 26947–26954. [[CrossRef](#)]
31. Ohkuma, H.; Nakagawa, T.; Shizu, K.; Yasuda, T.; Adachi, C. Thermally activated delayed fluorescence from a spiro-diazafluorene derivative. *Chem. Lett.* **2014**, *43*, 1017–1019. [[CrossRef](#)]
32. Reddy, S.S.; Sree, V.G.; Gunasekar, K.; Cho, W.; Gal, Y.S.; Song, M.; Jin, S.H. Highly Efficient Bipolar Deep-Blue Fluorescent Emitters for Solution-Processed Non-Doped Organic Light-Emitting Diodes Based on 9,9-Dimethyl-9,10-dihydroacridine/Phenanthroimidazole Derivatives. *Adv. Opt. Mater.* **2016**, *4*, 1236–1246. [[CrossRef](#)]
33. Méhes, G.; Nomura, H.; Zhang, Q.; Nakagawa, T.; Adachi, C. Enhanced Electroluminescence Efficiency in a Spiro-Acridine Derivative through Thermally Activated Delayed Fluorescence. *Angew. Chem.* **2012**, *51*, 11311–11315. [[CrossRef](#)] [[PubMed](#)]
34. Cho, A.N.; Chakravarthi, N.; Kranthiraja, K.; Reddy, S.S.; Kim, H.S.; Jin, S.H.; Park, N.G. Acridine-based novel hole-transporting material for high efficiency perovskite solar cells. *J. Mater. Chem. A* **2017**, *5*, 7603–7611. [[CrossRef](#)]
35. Romain, M.; Tondelier, D.; Jeannin, O.; Geffroy, B.; Rault-Berthelot, J.; Poriel, C. Properties modulation of organic semi-conductors based on a donor-spiro-acceptor (D-spiro-A) molecular design: New host materials for efficient sky-blue PhOLEDs. *J. Mater. Chem. C* **2015**, *3*, 9701–9714. [[CrossRef](#)]
36. Wang, Y.K.; Sun, Q.; Wu, S.F.; Yuan, Y.; Li, Q.; Jiang, Z.Q.; Liao, L.S. Thermally Activated Delayed Fluorescence Material as Host with Novel Spiro-Based Skeleton for High Power Efficiency and Low Roll-Off Blue and White Phosphorescent Devices. *Adv. Funct. Mater.* **2016**, *26*, 7929–7936. [[CrossRef](#)]

37. Romain, M.; Tondelier, D.; Geffroy, B.; Shirinskaya, A.; Jeannin, O.; Berthelot, J.R.; Poriel, C. Spiro-configured phenyl acridine thioxanthene dioxide as a host for efficient PhOLEDs. *Chem. Commun.* **2015**, *51*, 1313–1315. [[CrossRef](#)] [[PubMed](#)]
38. Jäger, L.; Schmidt, T.D.; Brütting, W. Manipulation and control of the interfacial polarization in organic light-emitting diodes by dipolar doping. *AIP Adv.* **2016**, *6*, 095220. [[CrossRef](#)]
39. Hu, N.X.; Xie, S.; Popovic, Z.D.; Ong, B.; Hor, A.M. Novel high Tg hole-transport molecules based on indolo [3,2-b] carbazoles for organic light-emitting devices. *Synth. Met.* **2000**, *111*, 421–424. [[CrossRef](#)]
40. Poriel, C.; Berthelot, J.R. Structure-property relationship of 4-substituted-spirobifluorenes as hosts for phosphorescent organic light emitting diodes: An overview. *J. Mater. C* **2017**, *5*, 3869–3897. [[CrossRef](#)]
41. Cho, Y.J.; Kim, O.Y.; Lee, J.Y. Synthesis of an aromatic amine derivative with novel double spirobifluorene core and its application as a hole transport material. *Organ. Electron.* **2012**, *13*, 351–355. [[CrossRef](#)]



© 2018 by the authors. Licensee MDPI, Basel, Switzerland. This article is an open access article distributed under the terms and conditions of the Creative Commons Attribution (CC BY) license (<http://creativecommons.org/licenses/by/4.0/>).